Evaluating the Trend and Impact Factors of Southeast Asian Monsoon

by

Warittha Panasawatwong

S.B., Massachusetts Institute of Technology (2018)

Submitted to the
Department of Earth, Atmospheric, and Planetary Sciences
Massachusetts Institute of Technology
in partial fulfillment of the requirements for the degree of

Master of Science in Atmospheric science

at the

MASSACHUSETTS INSTITUTE OF TECHNOLOGY

September 2018

Signature redacted

Author . . . .
Department of Earth, Atmospheric, and Planetary Sciences
Massachusetts Institute of Technology
August 31, 2018

Signature redacted

Certified by . . . .
Chien Wang
Senior Research Scientist of Earth, Atmospheric, and Planetary Sciences
Thesis Supervisor

Signature redacted

Accepted by . . . .
Rob van der Hilst
Schlumberger Professor of Earth and Planetary Sciences
Department Head of Earth, Atmospheric, and Planetary Sciences

Evaluating the Trend and Impact Factors of Southeast Asian Monsoon

by

Warittha Panasawatwong

Submitted to the Department of Earth, Atmospheric, and Planetary Sciences
Massachusetts Institute of Technology
on August 31, 2018, in partial fulfillment of the
requirements for the degree of
Master of Science in Atmospheric science

Abstract

As a global leading agricultural producer, Southeast Asian (SEA) economy and livelihood rely on water supply from the monsoon precipitation during the rainy season. However, SEA monsoon system is still understudied. Here, we focus on the Mainland SEA monsoon because of its geographical simplicity. We find that the total precipitation of the Mainland SEA monsoon has experienced a reversing trend from a four-decade-long drying by 0.18 mm day^{-1} decade^{-1} to increasing by 0.13 day^{-1} decade^{-1} starting from 1989. The increased energy and moisture post-reversal comes from the strengthened Hadley and Walker cell due to the increasing meridional equivalent potential temperature (θ_e) gradient. The meridional θ_e gradient shows significant correlation with the precipitation time-series at r = 0.52 (p = 0.0015), despite θ_e gradient has reversed ahead of precipitation for 4-5 years.

Even though the overall precipitation trend of Mainland SEA in recent decades is increasing, the north of Myanmar and the south of China shows a decreasing trend. The surface wind analysis shows that surface southwesterly is weakening in the Northern Hemisphere, so the north of Mainland SEA receives less moisture, but also allow more moisture from the South China Sea to access the south of Mainland SEA. The surface wind change also corresponds with the rising branch of Hadley cell shifting southward.

Lastly, we find that the Mainland SEA monsoon is a mixed convection system, composing of deep, moist convection directly over the region at 10-20°N, and a shallow, dry convection just north of the region at 35°, aligning with further assessment using zonal-mean precipitation, θ, and θ_e. The deep, moist convection coincides with the zonal-mean θ_e peak, and the strongest convection corresponds with the zonal-mean precipitation peak. The shallow, dry convection coincides with the zonal-mean θ peak.

Thesis Supervisor: Chien Wang

Title: Senior Research Scientist of Earth, Atmospheric, and Planetary Sciences

Acknowledgments

I would like to thank **Prof. Chien Wang**, my thesis advisor, for his continuous support and guidance throughout the duration of this research, and ultimately inspire me as a researcher. Thank you for trusting in me and my potential even when I don't. Thank you for giving me and this thesis this opportunity. This thesis also cannot take its final form without the help from **Prof. Paul O'Gorman** and **Prof. Tim Cronin**, members of this thesis committee. Thank you for helping me in multiple ways related to this research. Also, thank you **Dr. Qinjian Jin** for all the help in coding with NCL!

I also would like to thank those who support me for this past year of my Master's Program. Thank you Sika Gadzanku, Xiawei Liao, and Lik Khian Yeo, for all the talk in our office(s). Thank you members of MIT Pistol Team for all the positivity and love. Thank you Ju Chulakadabba, Ben Rak-amnouykit, Mee Tangpeerachai, and other members of Thai Student at MIT clubs for all the encouragement and support. Last but not least, thank you Paul Chonpimai and Katie Silva for being my eternal emotional support!

THIS PAGE INTENTIONALLY LEFT BLANK

Contents

List of Figures

List of Tables

THIS PAGE INTENTIONALLY LEFT BLANK

Chapter 1

Introduction

Southeast Asia (SEA) is located just south of China and spans to just south of the Equator. The region houses over 640 million people. Thanks to its advantageous tropical climate and abundant water supply during the rainy season, agriculture account a significant fraction in many countries' economy, such as 24.8% of their GDP in Myanmar (Central Intelligent Agency, 2018), and put themselves a global leading agriculture goods exporter. Water does not only serve as a necessity but also the backbone of its economy, affecting annual income for millions and food price in the market.

SEA water supply relies on the rain. The region does not have glacier melts or large lake as its reservoir. SEA water supply solely comes from rainfall during its rainy season, which characterized by the onset and the end of monsoon season. The change in monsoon precipitation each season affects the amount of water they have each year, unavoidably affecting their economy for the whole year. The monsoon extremity also causes droughts and floods. The increasing frequency of floods in recent decades has caused millions of dollars and thousands of lives in SEA (Loo, Billa, and Singh, 2015). Monsoon research is crucial for the development of SEA countries.

First, we need to understand the nature of the monsoon system. The simple monsoon model is similar to the sea breeze. The different heat capacities of land and sea create the thermal gradient. The air over the warmer land rises and cool air over the sea flows in, creating sea breeze that brought in moisture from over the sea to land. The moisture then precipitates as monsoon rain (Webster and Fasullo, 2003). However, the monsoon's spatial scale is larger than the sea breeze, and its onset is more sudden than sea breeze's subtle seasonal thermal gradient change. Monsoon system requires larger and stronger wind circulation system, called Hadley circulation. Hadley circulation or Hadley cell is a large-scale tropical circulation in tropics on both hemispheres with air converging toward then rising near equator. During boreal spring, the Hadley cells are almost symmetrical over the equator. Shifting into the boreal summer, air converge toward and rises on the Northern Hemisphere (NH) side, so one of the cell become cross-equatorial. In the cross-equatorial cell, air sinks in the Southern Hemisphere (SH) side, flows to the NH over the surface and rises in the NH. The shift of Hadley circulation corresponds with the seasonal shift of maximum heated area on the globe from over the equator to 20N in the summer. The shift of Hadley cell kickstarts the monsoon onset, and the single, cross-equatorial Hadley cell provides the large-scale surface winds to sustain the monsoon throughout its season (Bordoni and T. Schneider, 2008).

SEA monsoon also operates under the thermodynamics of Hadley circulation and thermal gradient, with some nuance due to its local geography. SEA monsoon is a sub-system of a larger monsoon system called the Asian-Australian monsoon system, which also includes the Indian monsoon, East Asian monsoon, and Australian monsoon. The SEA monsoon actually composed of two systems: The Mainland and Maritime SEA monsoon. In this study, we will focus on the Mainland SEA monsoon system because it is simpler to study than Maritime SEA for two reasons. First, because the monsoon precipitation is driven by thermal gradient between land and sea, Maritime SEA's complex islands-and-sea geography makes the monsoon temporal and spatial pattern complicated. On the other hand, Mainland SEA is composed simply and largely of the Indochinese Peninsula, making the thermal gradient and the wind simpler. Second, because the monsoon system onset is related to the shift of Hadley cell from almost symmetrical over the equator to asymmetrical with one dominant cell crossing the equator, the latitude of a system also determines the simplicity of the system. Mainland SEA locates from 5N and up, while Maritime SEA lays across the equator. Maritime SEA is then subjected to more complicated circulation shift than Mainland SEA.

Moreover, Mainland SEA monsoon system also has not been adequately explored. It is sometimes undermined as a branch of Indian monsoon system (the textbook monsoon, with rich literature precedent), and thus understudied despite the needs for agriculture planning, economic development, and quality of life improvement. We deem the Mainland SEA monsoon to be worthy of further investigation and therefore, we will focus on the Mainland SEA monsoon system.

Over the past decades, precedent researches in Mainland SEA monsoon precipitation shows a decreasing trend in 1950-1999 (Bollasina, Ming, and Ramaswamy, 2011), and overall increasing trend in 1970-2014 in the South of Mainland SEA (Preethi et al., 2017). The recent increase of monsoon precipitation corresponds with the recent increasing frequency of floods in SEA (Loo, Billa, and Singh, 2015), which causes damaging not only to the economics but to millions of residents in the region. Thus, the questions we want to explore in this study is on the multi-decadal variability of the Mainland SEA monsoon precipitation.

The recent increasing monsoon precipitation trends in the SEA is not unique to the region. The NH monsoon precipitation also shows increasing trend in the past 40 years (B. Wang et al., 2013). The speculating cause is inevitably on global warming, which can influence the Hadley circulation and subsequently monsoon precipitation. Simple thermodynamics predicts that the overall warming of the global surface should weaken the circulation (Held and Soden, 2006, Vecchi et al., 2006). However, observations show there are different heating rates in the NH and SH, with the NH warming faster than the SH in the past 40 years, creating the stronger thermal gradient and strengthening the monsoon circulation. This recent increasing thermal gradient along with other factors such as El Nino-Southern Oscillation (ENSO), explains the increasing precipitation trends over the past 40 years (B. Wang et al., 2013). However, the thermal gradient has not always been increasing. The gradient was decreasing but reversed to increase in the 1980s, as well as the NH monsoon circulation (figure 1-1).

The reversal explains previously found drying monsoon trend (H. Wang, 2001; Yu, B. Wang, and Zhou, 2004; Bollasina, Ming, and Ramaswamy, 2011). The NH monsoon precipitation likely went under the reversal in the 1980s following the reversal of the monsoon circulation trend. Locally, the reversal of precipitation trend has been identified in Indian summer monsoon to be in 2002 (Jin and C. Wang, 2017)

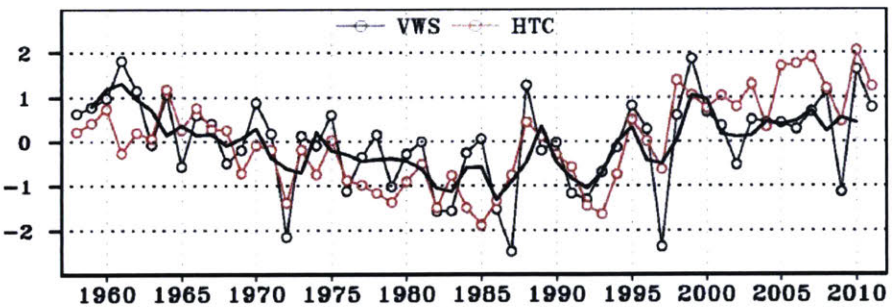

Figure 1-1: Normalized NH vertical wind shear (VWS), normalized hemispheric thermal contrast (HTC, red). Vertical wind shear, measured by 850-hPa minus 200-hPa winds and averaged over 0–20°N, 120°W–120°E, acts as NH summer monsoon circulation index. Normalized HTC index measured by the 2-m air temperature averaged over the NH (0–60°N) minus that over the SH (0–60°S), significantly correlates with VWS (r = 0.63). The thick black line shows 3-year running means of NH monsoon circulation index. Computed from merged ERA-40 (1958–1978) and ERAI (1979–2011) reanalysis datasets. Adapted from Wang et al. (2013) with Copyright (2013) National Academy of Sciences.

Thus, in this study, we will explore the Mainland SEA monsoon system and its precipitation trend and variability particularly in recent decades. In chapter 2 we will first analyze the Mainland SEA monsoon precipitation and its multi-decadal variability, by computing area-averaged precipitation time-series. We will also examine the spatial distribution of monsoon precipitation and its trend. In chapter 3, we will analyze the mean surface wind, and zonal- and meridional-mean circulation of the Mainland SEA monsoon system, and explore whether the circulation system corresponds with the observed spatial precipitation pattern. In chapter 4, we will explore the local thermal gradient, by creating the map of mean temperature, and evaluate whether it could explain the monsoon circulation system as analyzed in chapter 3. We will compute zonal-mean temperature parameters We will also compute the thermal gradient time-series and its correlation with the precipitation time-series, to evaluate whether it shows a similar correlation as shown in the large-scale NH monsoon system. Lastly, the major results of this study will be summarized in chapter 5.

THIS PAGE INTENTIONALLY LEFT BLANK

Chapter 2

Precipitation Trend of Sea Monsoon in Recent Decades

Precedent researches in Mainland SEA monsoon precipitation show a decreasing trend in 1950-1999 (Bollasina, Ming, and Ramaswamy, 2011), and overall increasing trend in 1970-2014 in the South of Mainland SEA (Preethi et al., 2017). Thus, there is a discontinuity in the detailed precipitation trend specifically in recent several decades. Therefore, in this chapter, we aim to analyze the Mainland SEA monsoon precipitation trend and its variability. We will first describe the datasets used to compute the precipitation time-series. Then, we will compute the statistical monthly mean precipitation, to select pre-monsoon and monsoon season. Precipitation's spatial pattern of pre-monsoon and monsoon season is then plotted and analyzed. Next, the yearly-mean precipitation during monsoon season is plotted to evaluate trend and variability. Lastly, we will plot and analyze the spatial distribution of the precipitation trend.

2.1 Precipitaion Datasets

Five gridded observed precipitation datasets are used to compute the precipitation trend. The datasets are: CRU TS v.4.00 ($0.5° \times 0.5°$) from Climate Research Unit

(CRU) of East Anglia (Harris et al., 2014), GPCC V7 ($1°\times1°$) from Global Precipitation Climatology Centre (U. Schneider et al., 2014), PREC/L50 ($1°\times1°$) from US National Oceanic and Atmospheric Administration (NOAA) (Chen et al., 2002), Global Precipitation Climatology Project (GPCP) version 1.2 ($2.5°\times2.5°$) (Adler et al., 2003), and the Tropical Rainfall Measuring Mission (TRMM) version 3B43 ($0.25°\times0.25°$) (Huffman et al., 2007).

CRU TS precipitation is based on over 5,000 station records. The GPCC V7 precipitation product is based on 67,200 rain gauge stations. PREC/L global precipitation is based from over 17,000-gauge observations over land. GPCP v1.2 merged data from rain gauges, satellite retrievals, and sounding observations. TRMM 3B43 merged the satellite retrieved precipitation using microwave data, infrared radiance, and other satellite data as well as selected surface rain gauge station data. Due to the inclusion of satellite data in GPCP and TRMM, these datasets do not go back as long as the other three. CRU and GPCC have the data available from 1901, and PREC/L from 1948. While GPCP dataset starts their time-series in 1979, and TRMM datasets start in 1998. Therefore, for evaluation that requires longer time-series, only CRU, GPCC and PREC/L will be used.

2.2 Pre-Monsoon and Monsoon Seasons

In order to select only the precipitation that is related to monsoons, we need to analyze the time window of the monsoon season. Thankfully, the majority of Mainland SEA precipitation is due to monsoons, so its rainy season is the monsoon season. The start of the rainy season then corresponds with the onset of the monsoon, which falls at the beginning of May to mid-June (Kiguchi et al., 2016). Thus, we define the pre-monsoon season to be May-June. For monsoon season, we select the months where precipitation clearly peak compared with other months. In figure 2-1, we compute the long-term monthly mean from 1948-2016 precipitation datasets. It shows that the precipitation increases sharply in May and June, corresponding with the monsoon onset. The precipitation then continues to increase from June to August, then starts to drop in

September. September mean precipitation is still relatively large, compared with the sharp drop in October. Thus, we define the monsoon season to be June-September.

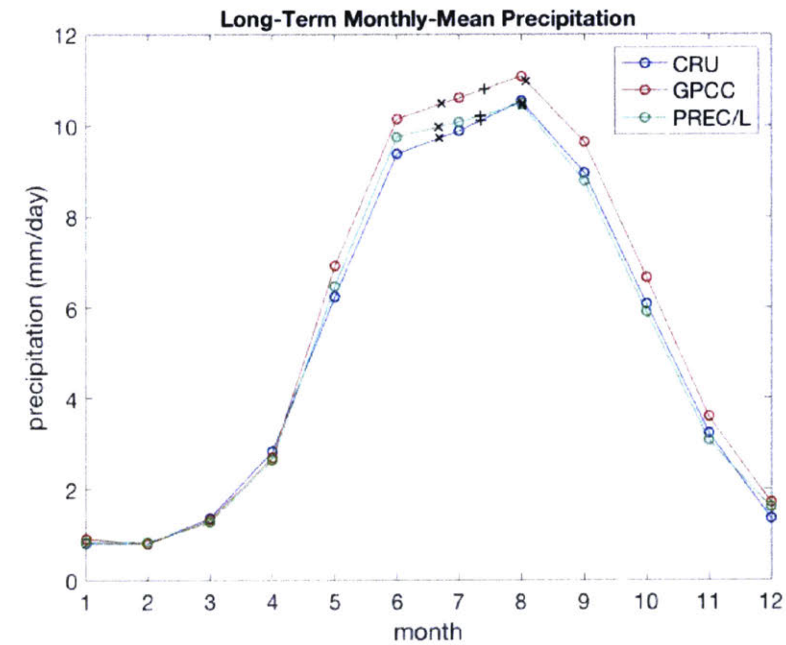

Figure 2-1: Long-term monthly-mean precipitation from 1948-2016. The monsoon season is from June to September, with peak precipitation in August. Precipitation's mean falls roughly on July 12, and the standard deviations fall roughly on June 22 and August 2. The mean day of precipitation distribution is shown in plus sign, and the standard deviation is shown in cross sign. Computed in the area of 5-25°N and 90-110°E, using CRU, GPCC, and PREC/L datasets.

2.3 Precipitation Spatial Pattern during Pre-Monsoon and Monsoon Seasons

Geography, such as mountain ranges, introduces spatial deviation for precipitation. The spatial difference is especially important for local government to assess different needs, and for researchers to assess the system further. We will later look at the relationship between the surface wind and the precipitation spatial pattern. The spatial pattern serves as the checkup point for consistency between datasets.

We compute mean precipitation during pre-monsoon and monsoon season for each dataset from 1948-2016. As shown in figure 2-2, the heaviest precipitation falls in the west coast, the west side of the Indo-Malayan mountain system which runs from the north of Myanmar to the south of Thailand, for both pre-monsoon and monsoon season. There is a clear difference between the precipitation on the west side and the east side of the Indo-Malayan mountains. During monsoon season, the precipitation intensity in the east side of the Indo-Malayan mountain increases, especially around the Mekong River Basin, albeit still not as strong as in the west coast. The precipitation's spatial pattern is consistent among the three datasets.

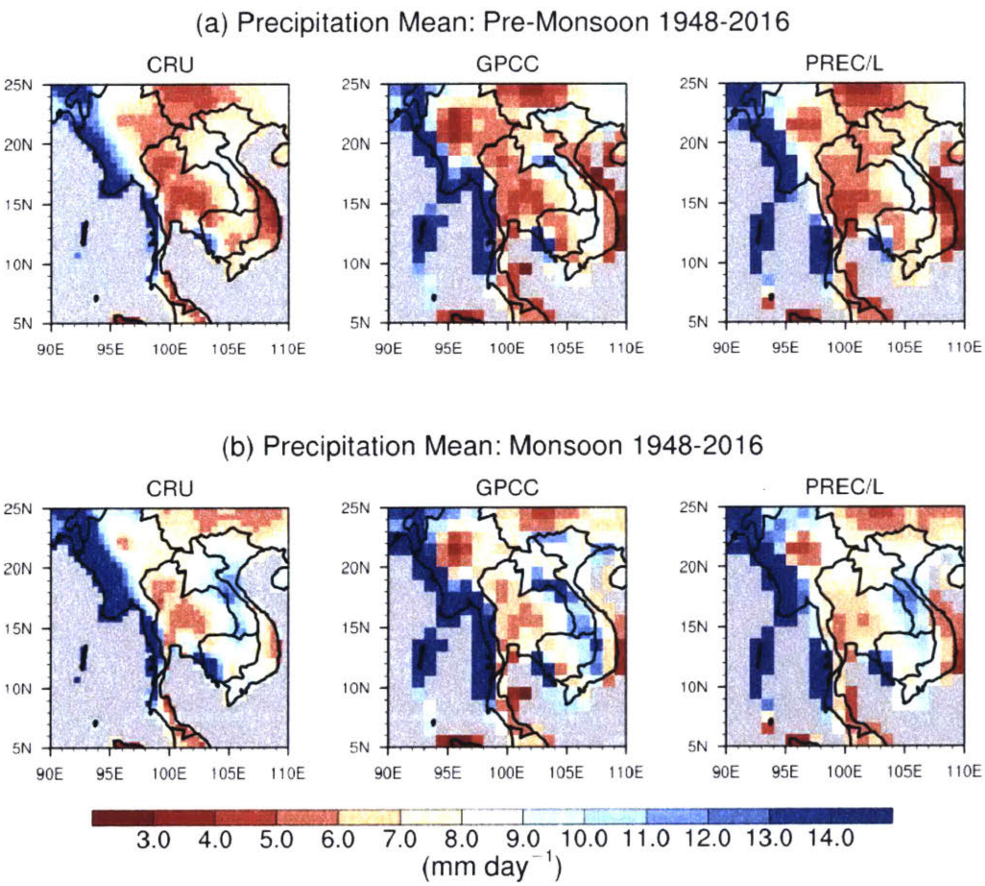

Figure 2-2: The spatial pattern of precipitation means of monsoon precipitation in 1948-2016. The geographical influence of the Indo-Malayan mountain system is apparent, as the precipitation intensity drops from the west side to the east side of the mountains.

2.4 Precipitation Trend and Variabilities

To examine the precipitation trend and its variability, we computed the total precipitation in Mainland SEA during monsoon season for each year from 1948-2016. The time-series show decadal variability, possibly correlated with the ENSO. However, there is also a multi-decadal variability. The time-series shows an overall decreasing from 1948, but reverse to increasing trend over the recent several decades. However, the reversing year is not clear. The possible turning point could be either 1989 or 1999, where the precipitation drops to local minima, because of a sharp precipitation peak in 1995.

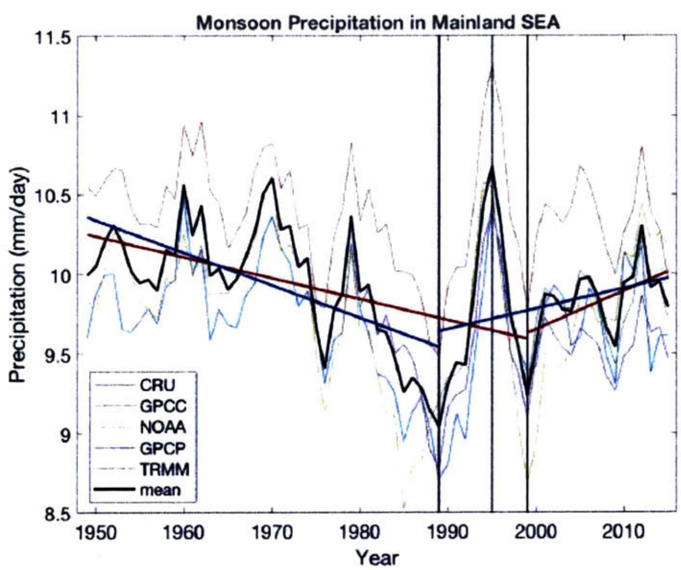

Figure 2-3: Total precipitation intensity during the monsoon season from 1948-2016 from 5 observation datasets, with the year 1989 and 1999 marked as the possible reversal year. Blue lines mark the trend if the reversal is in 1989 and red lines mark the trend if the reversal is in 1999.

We evaluate the reversal year by applying trend analysis to before and after each possible reversing year, then select the reversing year from the significant level of the trends. The trend analysis is shown in table 2.1. Using 1989 as the reversing year yields a lower p-value for the trend pre- and post-reversal. Thus, we will use 1989 as the reversing year for further analysis

Reversing Year	Pre-Reversal		Post-Reversal	
	Trend (dec^{-1})	MK, p-value	Trend (dec^{-1})	MK, p-value
1989	-0.18 mm day^{-1}	0.001	0.13 mm day^{-1}	0.186
1999	-0.13 mm day^{-1}	0.004	0.12 mm day^{-1}	0.325

Table 2.1: The trend analysis of precipitation (1948-2016) for pre- and post-reversal of 1989 and 1999 as possible reversing year.

2.5 Spatial Pattern of Precipitation Trend Pre- and Post-Reversal

Even though the trend of overall precipitation in Mainland SEA is analyzed, the trend may still not be consistent throughout the region. Thus, we compute the precipitation trend for pre- and post-reversal (using 1989 as reversing year) for each point in the datasets. The spatial pattern is plotted in figure 2-4.

The most severe reversal happened along the west coast of Northern Myanmar, which were the area with the highest precipitation (figure 2-2). The west coast went from having the strongest decreasing trend pre-reversal to the strongest increasing trend post-reversal. CRU and PREC/L also picked up a reversal of similar degree in Southern Myanmar. Even though GPCC does not show the same extreme increasing trend post-reversal (which might be the result of low resolution), the three datasets agree on the significant reversal from decreasing to increasing trend in Central Thailand.

On the other hand, the opposite reversal happened in Northern Myanmar and Southern China, going from having increasing precipitation trend to decreasing after the reversal. In Northern Myanmar, CRU and GPCC shows the increasing trend pre-reversal significant, while PREC/L shows decreasing trend-post reversal significant, and might prone to signify drying trend pre- and post-reversal than others. Moreover, PREC/L post-reversal trend pattern is also not as spatially consistent as the other two datasets, which might also be the result of low resolution.

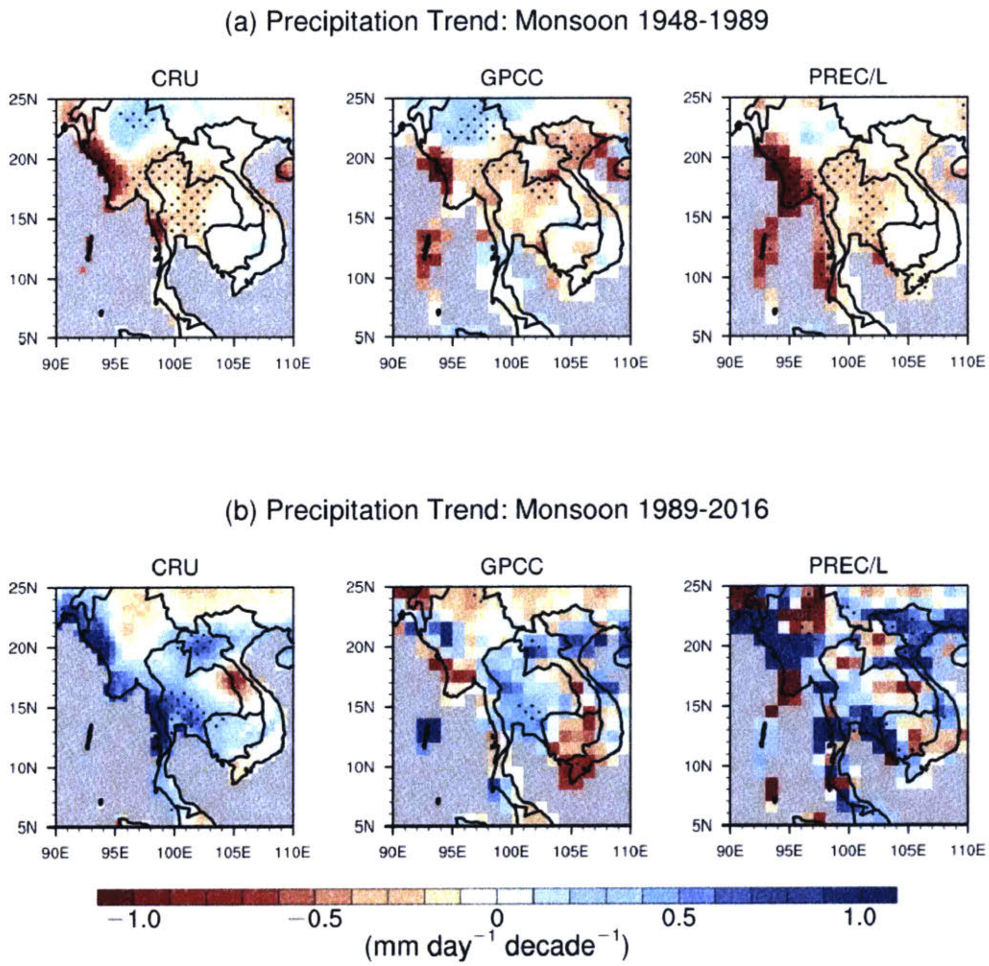

Figure 2-4: The spatial pattern of linear trends of precipitation (mm d-1 decade^{-1}) during (a) pre-reversal in 1948-1989 and (b) post-reversal in 1989-2016. The black dots indicate trends that are confident at 95% level.

2.6 Summary

We found that there is a reversal in the Mainland SEA monsoon precipitation trend around or immediately after 1989, turning from a nearly half-century long drying to a drastic wetting. This reversal is about a decade later than the NH monsoon reversal, but earlier than the Indian monsoon reversal. It is not clear how long this recent multi-decadal wetting will persist. If the trend persists, the majority of the Mainland SEA will need to improve its water management structure for the increased precipitation and its subsequent disasters, i.e. floods and landslides. While the north of Myanmar and the South of China will face persistent drought.

Chapter 3

SEA Monsoon Circulation

The summer monsoon onset has been associated with the shift of Hadley cells from almost symmetric over the equator to one dominant cross-equatorial cell (Bordoni and T. Schneider, 2008). The monsoon is then driven within the cross-equatorial Hadley circulation. Here we will first describe the data used to analyze the wind circulation. Then, we will analyze the surface wind in relation to the spatial pattern of precipitation, and then the zonal- and meridional-mean of horizontal and vertical wind, as well as inspect the change in the system after the reversal of precipitation trend

3.1 Datasets

The wind datasets used in this chapter are wind speed at surface as well as 17 pressure levels (1,000-10 mbar) from US National Center for Environmental Prediction (NCEP) and National Center for Atmospheric Research (NCAR) reanalysis ($2.5° \times 2.5°$) (Kalnay et al., 1996). However, in the actual zonal- and meridional-mean wind cross-section analyses, we only use the pressure levels wind from 1,000 to 150 mbar. The datasets are available from 1948-2017.

3.2 Surface Wind

The surface wind is a part of the dynamics that brought in the moisture from over the sea to inland. The spatial distribution of precipitation is inevitably affected by the combination of geography and surface wind pattern. Here, we compute the mean of surface wind during pre-monsoon and monsoon season 1948-2014, shown in figure 3-2. The general wind direction is similar in both seasons, but the monsoon wind is slightly stronger than pre-monsoon wind. The zonal wind direction changes from easterly in 5-25°S to westerly in 0-20°N, due to Coriolis effect. However, the meridional wind is generally southerly, corresponding with the cross-equatorial Hadley circulation. Tracing back the streamline of surface wind, we can find the moisture source of Mainland SEA monsoon to be from the Bay of Bengal and the Indian Ocean in SH. Over Mainland SEA, the wind flowing in is southwesterly, corresponds with the precipitation's spatial distribution (figure 2-2) that the precipitation is higher on the west side of the Indo-Malayan mountains and the precipitation then drops sharply on the lee side of the mountains.

Then, we compute the mean wind change from pre- to post-reversal for pre-monsoon and monsoon season, by subtracting the mean surface wind of 1989-2017 with the mean surface wind of 1948-1989 (figure 3-2). The result shows that the wind in the NH generally become more northerly, while the wind in the SH, especially near the equator, becomes more southerly. For Mainland SEA, this means the southwesterly from Bay of Bengal has weakened, and moisture is not carried far in land as before. The change reflect in the north of Myanmar and the south of China's drying trend, where the area is farther in land. In the same time, the northeasterly anomaly over the South China Sea allows more moisture to access the south of Indochinese Peninsular, corresponding with the wetting trend in the rest of Mainland SEA. However, the weakening landward wind from the Bay of Bengal does not correspond with the significantly increasing trend along the west coast of the peninsula.

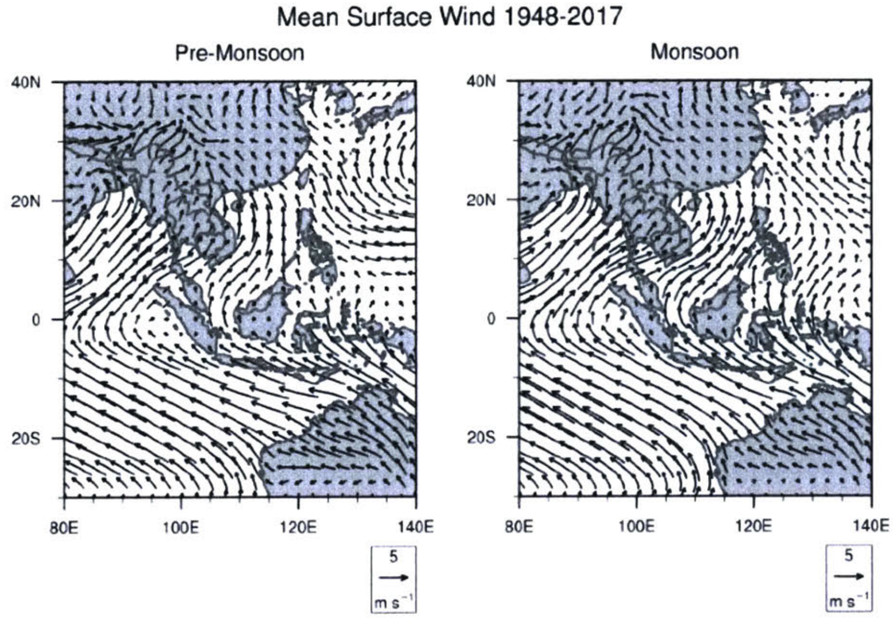

Figure 3-1: Mean surface wind during pre-monsoon and monsoon 1948-2014. The general direction of the wind is similar, but the monsoon wind is slightly stronger than pre-monsoon. The reference wind is 5 m s^{-1}.

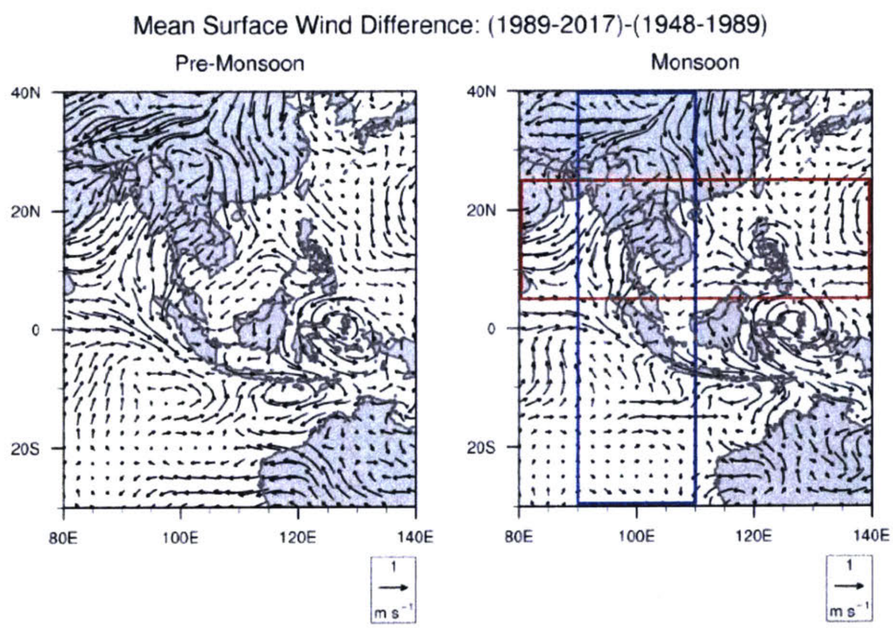

Figure 3-2: Mean surface wind difference from pre- to post-reversal, computed from the mean surface wind of 1949-1989 subtract from the mean of 1989-2014 for each season. The reference wind is 1 m s^{-1}. The blue and red box mark the area used to compute the zonal- and meridional-mean in section 3.3.

3.3 Zonal- and Meridional-Mean Wind Cross-Section

Monsoon system does not only consist of horizontal flows but also vertical wind. As the monsoon circulation resides within the large-scale Hadley circulation, it is important to look at the large-scale vertical convection together with the horizontal flows to understand the monsoon dynamics, location, and intensity.

The monsoon convection system can be divided into two types: the deep convection system, and the mix between deep, moist convection and shallow, dry convection system (Nie, Boos, and Kuang, 2010). By taking the zonal mean of meridional and vertical wind over each monsoon region during monsoon season, we can analyze the convection type of each regional monsoon system. The deep convection system, such as the Indian monsoon, has only one strong rising branch in the Hadley circulation. On the other hand, the mixed convective system, such as North African monsoon, has one strong rising branch and another smaller, shallower branch.

To inspect the convection of Mainland SEA monsoon system, we take the zonal mean of meridional and vertical wind over Mainland SEA during monsoon season 1948-2017. The result, as shown in figure 3-3, shows the large convection arises from 10 to 20°N, directly over Mainland SEA, and flows over the equator in the upper atmosphere. This convection branch is likely corresponding to the Mainland monsoon convection. There is also another convection resides within deep Hadley convection. This smaller system comprises of the air rising from the equator to the upper troposphere, flows southward, and starts sinking around 15°S near if not the same as the sinking branch of Hadley cell. This shallow convection is possibly due to the mass of lands in Maritime SEA and might be related to the Maritime-Continent Monsoon system. Still, the near-surface wind overall is driving cross-equatorial from SH to NH toward Mainland SEA. In the subtropics, there is another convection peaking at 30°N, but the rising is shallower, and the flow seems to join into the larger convection.

The meridional mean plot shows the near-surface wind driving eastward from the Bay of Bengal to the Indochinese Peninsula. The wind pattern also explains precipitation's spatial pattern (figure 2-2) and corresponds with the surface wind (figure 3-1), where the strongest precipitation is along the west coast of Myanmar, fully baring the wind from the Bay of Bengal.

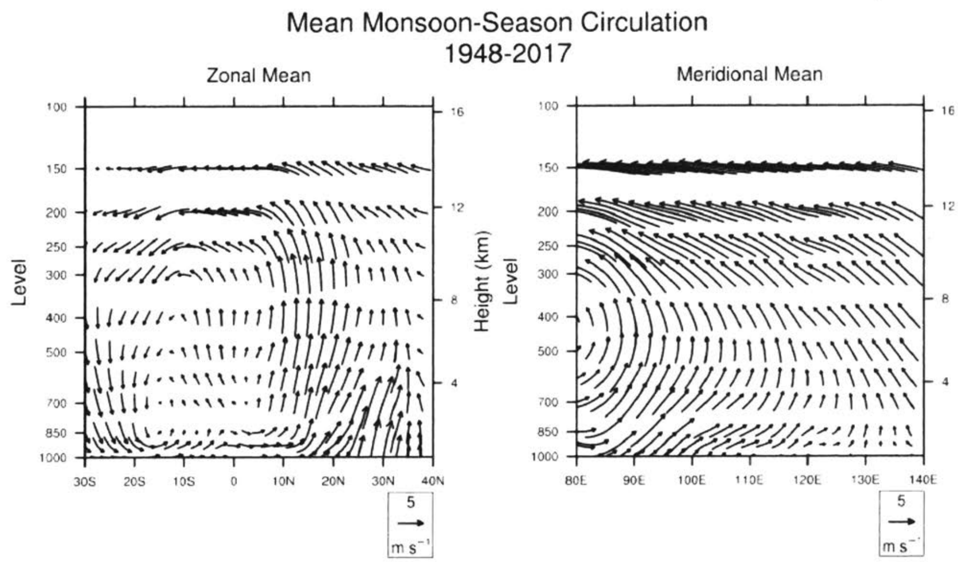

Figure 3-3: Mean wind during monsoon season 1948-2016. Computed from NCEP reanalysis dataset. The zonal mean is taken from the coordinates of 5-25°N, 80-140 °E, marked by blue box in figure 3-2. The meridional mean is taken from the coordinates of 30°S-40°N, 90-110°E, marked by red box in figure 3-2. The vertical velocity is multiplied by 100 for visibility in the plot. The reference vector is 5 m s^{-1}.

To inspect the circulation change after the reversal of the precipitation trend, the mean monsoonal wind from pre-reversal (1948-1989) is subtracted from the mean monsoonal wind from post-reversal (1989-2017). As shown in figure 3-4, the zonal-mean change shows that the southward cross-equatorial flow in the upper troposphere is strengthened. Although the usual rising branch over 10-20°N is slightly weakening, the rising branch of the shallower circulation over the Maritime SEA on the equator is clearly strengthening, as well as the surface convergent toward the new rising branch. However, the cross-equatorial flows in the upper-troposphere does not show the divergence anomaly in respect to the rising branch over the equator. It maintains the direction and also strengthen its magnitude.

The meridional-mean of wind change also shows the strengthening of the Walker cell with two rising branches: one over the over the South China Sea and one over the Philippine Sea in the far east of the plot. The two rising branches join in the upper troposphere flow eastward. Near-surface, the easterly wind from the South China Sea is present, corresponding with the surface wind. On the other hand, both near-surface westerly wind and the rising branch from the Bay of Bengal is weakening. It corresponds with the surface wind change and likewise does not corresponding with the increasing precipitation trend on the west coast of the peninsula.

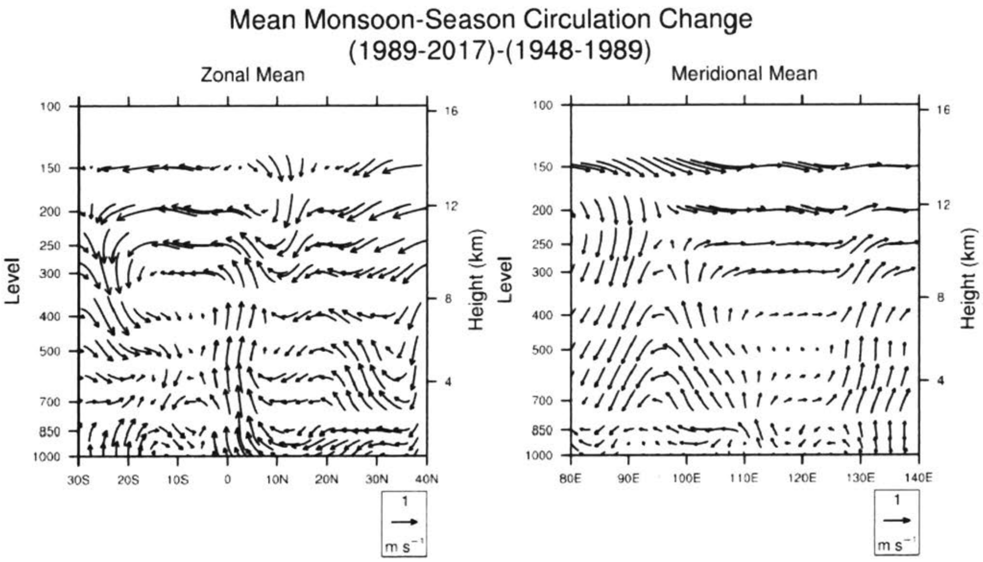

Figure 3-4: Changes in the mean wind during monsoon season before and after the reversal, with the mean of 1948-1989 subtracted from the mean of 1989-2017. Computed from NCEP reanalysis dataset. The zonal mean is taken from the coordinates of 5-25 °N, 80-140 °E, as marked in the blue box in figure 3-2. The meridional mean is taken from the coordinates of 30 °S – 40 °N, 90-110°E, marked in the red box in figure 3-2. The vertical velocity is multiplied by 100 for visibility. The reference vector is 1 m s^{-1}.

3.4 Summary and Discussions

The surface wind shows strong cross-equatorial southeasterly in SH and northeasterly in NH, bringing the air from the Indian ocean in SH and Bay of Bengal to Mainland SEA. The shift of the surface wind shows the weakening of the southerly wind in NH, especially in the north of SEA and south of China, explaining the drying in the area. On the other hand, the strengthened landward wind from the South China Sea explains the increasing precipitation other regions of SEA.

The cross-section wind analysis shows the Mainland SEA monsoon is like a mixed convection system, with a deep, moist convection over the Mainland SEA, and a shallow, dry convection in the subtropics. The cross-section wind change shows slight weakening of the usual rising branch of Hadley cell over Mainland SEA. However, another rising branch of the Hadley cell over the equator is strengthened, as well as the surface convergent toward the new rising branch. The cross-equatorial flows in the upper-troposphere is strengthened as well. Overall, the Hadley circulation seems to be strengthened. The Hadley cell's rising branch moving southward corresponds with precedent research on the southward shift of the Intertropical Convergence Zone (ITCZ) due to different anthropogenic aerosols distribution in the NH and SH (C. Wang, 2015; Chung and Soden, 2017).

Iwt is speculated that the anthropogenic aerosols and greenhouse gas weaken Hadley and Walker circulation, leading to weakening of South Asian monsoon. Bollasina, Ming, and Ramaswamy, 2011). Here, the change in circulation is in the opposite direction in recent several decades, and the precipitation trend is reversing from decreasing to increasing. Even though we cannot give conclusions about the change in anthropogenic aerosols and greenhouse gas, in this case, we can exhibit the relationship between the circulations and monsoon precipitation intensity.

THIS PAGE INTENTIONALLY LEFT BLANK

Chapter 4

Driver and Its Correlation With Precipitation

Thermal contrast is sometimes said to be the primary driver of monsoon dynamics, driving the surface wind and bringing the energy and moisture from over the oceans to inland during the monsoon season (Webster and Fasullo, 2003). The monsoon precipitation is found to be correlated with the pre-monsoon thermal gradient (Li and Yanai, 1996). However, the land-sea thermal contrast is found not to be the key driver for monsoon onset, as the gradual change of the thermal contrast does not explain the sudden nature of monsoon onset. On the other hand, the rapid transition of Hadley circulation from nearly symmetrical over the equator to one dominant cell rising in the NH is enough to produce monsoon-like precipitation even in aquaplanet simulations (Bordoni and T. Schneider, 2008). Still, the observed temperature parameter is related to the circulation dynamics. The zonal-mean equivalent potential temperature (θ_e), not sensible temperature, is found to qualitatively correspond with the vertical convection of the monsoon system (Nie, Boos, and Kuang, 2010). We will investigate the relationship the temperature has with monsoon precipitation and convection in this chapter. First, we will describe the datasets used to analyze temperature. Then, we will compute the yearly mean temperature time-series during pre-monsoon season, and investigate its correlation with monsoon precipitation. Lastly, we will analyze the zonal-mean potential temperature and equivalent potential temperature in relation to the zonal-mean circulation found in chapter 3.

4.1 Datasets

The surface temperature data is composed of sea surface temperature from HadISST ($1^{\circ}\times1^{\circ}$) from the Hadley Centre of UK Met Office (Rayner et al., 2003) and surface air temperature from University of Delaware ($0.5^{\circ}\times0.5^{\circ}$) (Legates and Willmott, 1990). The HadISST dataset is available from 1870-present. However, the UDel TS is only available from 1901-2014. Here, we will use select the time-series from 1948-2014, so the starting year is consistent with the precipitation datasets.

For the surface θ_e, we compute the surface specific humidity for land and sea differently. For over land, we compute surface specific humidity using available NCL package on monthly-mean surface pressure and dew-point temperature from the European Centre for Medium-Range Weather Forecasts (ECMWF) Re-Analysis ERA-interim ($0.75^{\circ}\times0.75^{\circ}$) (Dee et al., 2011). For over sea, we compute surface specific humidity according to Byrne and O'Gorman (2018). Firstly, the surface relative humidity is computed using available NCL package on ERA-interim's monthly-mean 2m temperature and dew-point temperature data, and average result for each month from 1979-2001. Then, we compute the specific humidity using the averaged monthly-mean relative humidity, and ERA-interim's surface pressure and 2m temperature data. Then, the surface θ_e is computed using available NCL package on the computed specific humidity, monthly-mean 2m temperature, and surface pressure from ERA-interim.

4.2 Thermal Gradient and Its correlation with Precipitation

The monsoon precipitation is found to be correlated with the pre-monsoon temperature gradient in the Indian monsoon (Li and Yanai, 1996). For thermodynamics to work, thermal gradient should have the land surface temperature higher than sea surface temperature. However, the simply observed temperature does not show the thermal contrast required to drive the monsoon in SEA (figure 4-1). The surface temperature over the Indochinese Peninsula is as warm as the sea surface temperature over the body of water surrounding it. The surface temperature up North over China is even cooler. However, if the monsoon onset does not require the land-sea thermal gradient as in 'sea breeze' model but instead the shift of the Hadley circulation, we can extend the spatial scale of thermal gradient from land-sea gradient to cross-equatorial meridional temperature gradient. The meridional gradient would correspond with the meridional surface wind in the Hadley cell. Still, the meridional temperature gradient is found to be relatively weak. Instead, we use the equivalent potential temperature θ_e which represents not only sensible heat but also the latent heat energy of the moisture in the air. The spatial pattern of θ_e shows required thermal gradient from the Indian ocean in SH over to Indochinese Peninsula, Bay of Bengal, and South China Sea (figure 4-2).

The change of θ_e is computed by subtracting the mean θ_e during 1989-2014 with the mean θ_e during 1948-1989. The plotted difference, shown in figure 4-3, shows that the land surface θ_e is overall warming faster than sea surface θ_e. Because the majority of the land is in the NH, we expect the θ_e in the NH to be warming faster than the θ_e in the SH. Therefore, the thermal gradient should be strengthened post-reversal. The land θ_e over the equator also warms faster than its neighbor. The local warming explains the strengthened convection over the equator (figure 3-4). However, because the wind analysis is from re-analysis dataset (NCEP) and we also use pressure and 2m dew-point temperature from re-analysis dataset (ERA-interim) to compute θ_e, it is possible that this could be the regional warming outlier that presents in both systems.

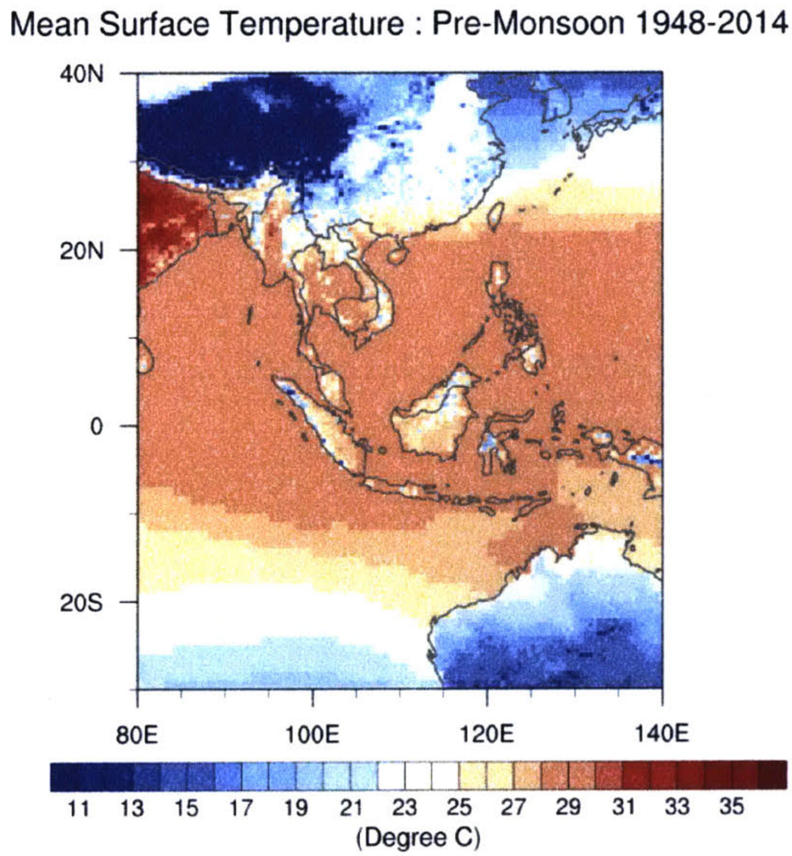

Figure 4-1: Mean surface temperature during pre-monsoon season 1948-2014. The land-sea temperature gradient is not strong enough to drive the monsoon onset. Using the merged of UDel for over land surface temperature and HadISST for sea surface temperature.

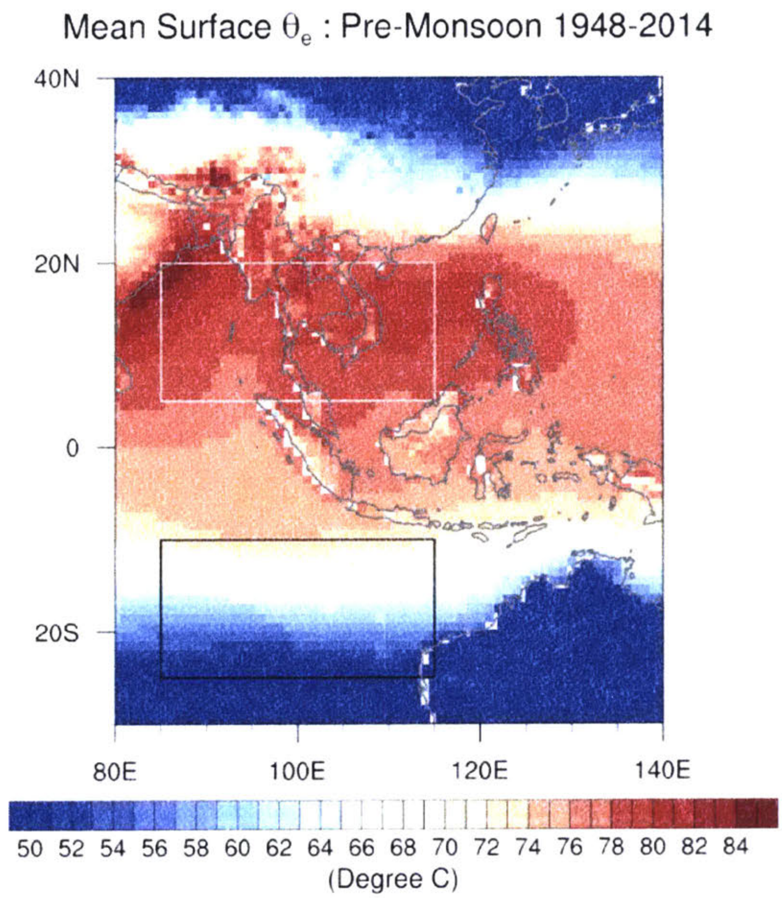

Figure 4-2: Mean equivalent potential temperature during pre-monsoon season 1948-2014. The meridional cross-equatorial thermal gradient is stronger. The white and black boxes show the area used to compute meridional θ_e gradient.

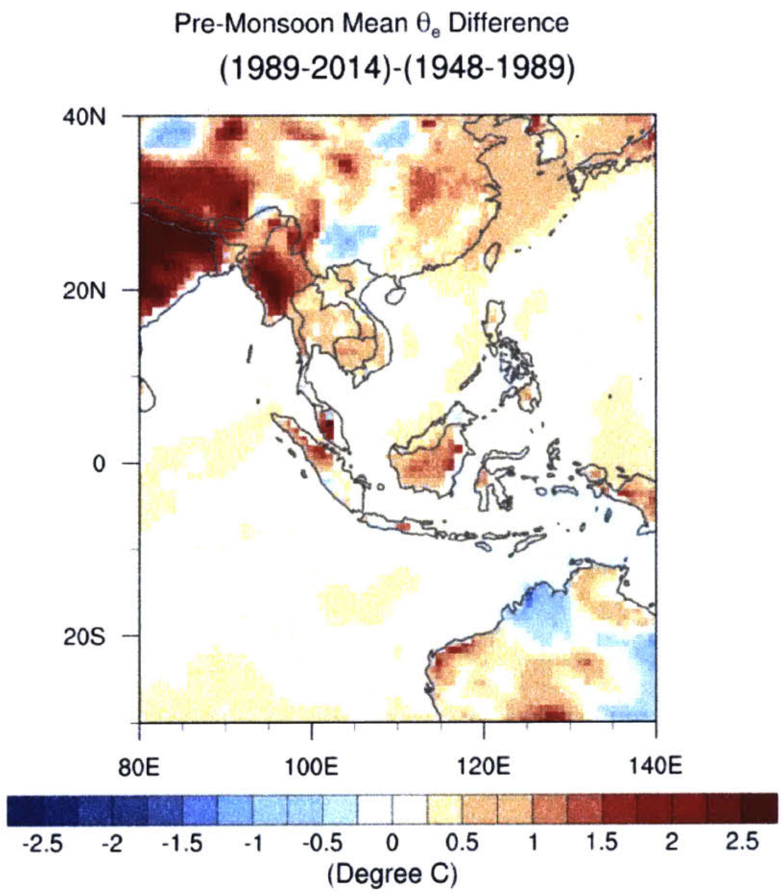

Figure 4-3: The spatial pattern of pre-monsoon surface θ_e difference between pre- and post-reversal. Computed by subtracting the pre-monsoon mean θ_e during pre-reversal (1948-1989) from the mean θ_e during post-reversal (1989-2017). The warming over land is faster than the warming over the sea.

We then compute the meridional surface θ_e gradient between the NH (5-20°N, 85-115 °E, marked by the white box in figure 4-2) and SH (5-25°S, 85-145°E, marked by the black box in figure 4-2). figure 4-4 shows the mean θ_e computed in each box. The SH θ_e which consists mostly of sea surface does not warm as the NH θ_e which has more land area, as expected. The NH θ_e increasing rate also accelerated in the last decade. If the trend persists, the thermal gradient would get even stronger, resulting in even more increasing precipitation. The θ_e gradient is then computed and plotted along with monsoon precipitation in figure 4-5. The θ_e gradient seems to have reversed in 1984-85, a couple years ahead of precipitation reversal in 1989. The two time-series show significant correlation of r = 0.52 (p = 0.0015).

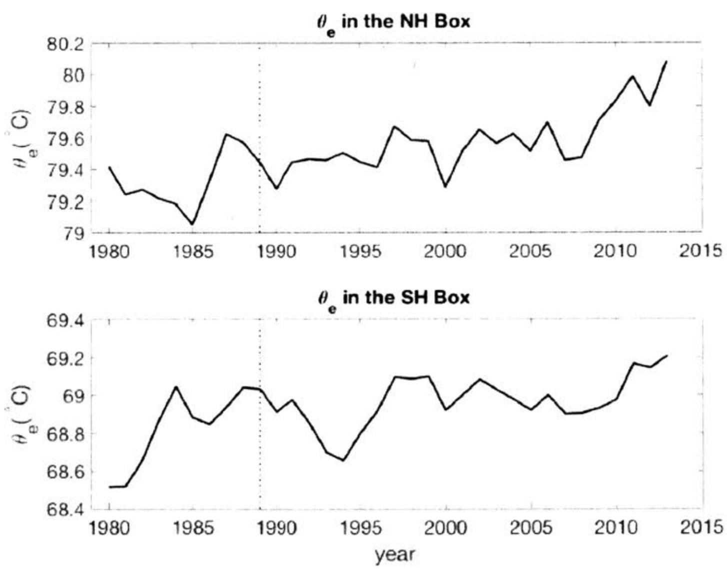

Figure 4-4: Mean surface θ_e computed in the NH box (5-20°N, 85-115 °E, marked by the white box in figure 4-2) and the SH box (5-25°S, 85-145°E, marked by the black box in figure 4-2). The reversing year 1989 is marked. The SH θ_e which consists mostly of sea surface does not warm as the NH θ_e which has more land area. The NH θ_e increasing rate also accelerated in the last decade.

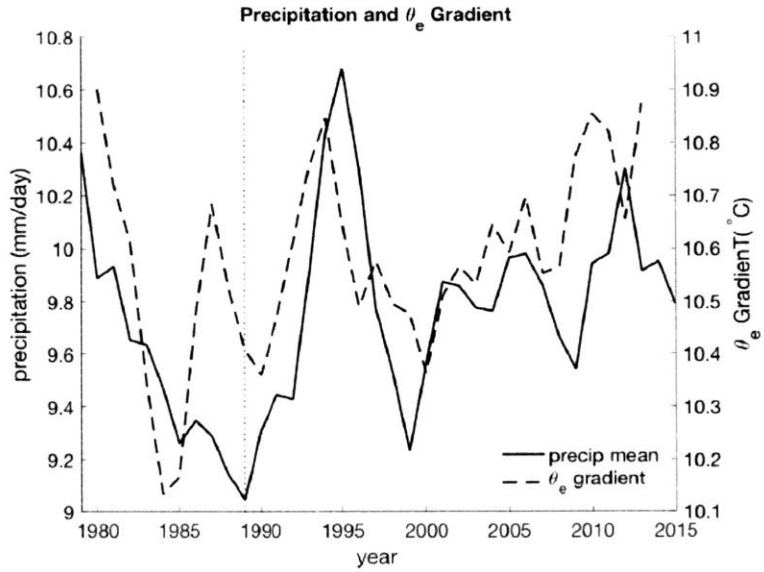

Figure 4-5: Pre-monsoon meridional θ_e gradient (dashed line) and total monsoon precipitation over Mainland SEA (solid line). The thermal gradient is in 1984-85, ahead of precipitation reversal in 1989. The correlation r = 0.52 (p = 0.0015).

4.3 Zonal-Mean Potential Temperature and Convection

It has been proposed that the depth of monsoon convention is reflected in the zonal mean of precipitation and potential temperatures (Nie, Boos, and Kuang, 2010). The deep, moist convection would correspond with near-surface θ_e and precipitation peak, and the shallow, dry convection would correspond with near-surface θ. From the zonal mean circulation (figure 3-3), the Mainland SEA monsoon is likely a mixed convection system with the deep, moist convection in 10-20°N and shallow, dry convection at around 35°N. To further attest to this model, the zonal mean precipitation, θ, and θ_e are computed and plotted in figure 4-6. The zonal-mean of θ and θ_e is rather not smooth because of the peninsula and islands nature of the region. Nevertheless, the zonal-mean parameters correspond with the convections in figure 3-3. The strongest wind in the deep, moist convection latitude coincides with the precipitation peak latitude. The zonal-mean θ_e peak spans from 10°S-30°N, and roughly corresponds with the overall deep convection branch from 10°S-20°N. However, the smaller convective peak over the equator does not show in the zonal-mean θ_e. The shallow, dry convection location corresponds with the zonal-mean θ peak at 35°N.

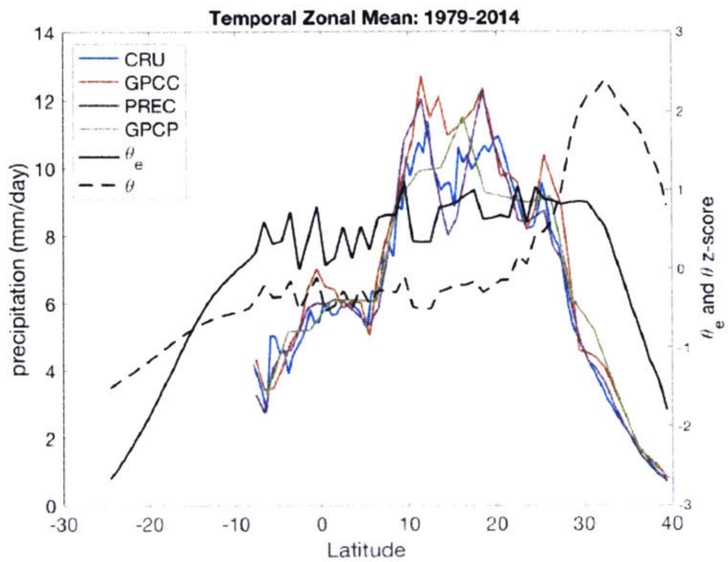

Figure 4-6: Zonal-mean of precipitation, θ, and θ_e during monsoon-season 1979-2014. The precipitation peak location of all four datasets corresponds with the strong wind peak (10-20°N) in the deep, moist convection in figure 8. The θ_e also roughly corresponds with the overall deep, moist convection (10°S-20°N), although the vertical wind peak over the equator does not show in the zonal-mean θ_e. The θ peak corresponds with the shallow, dry convection ($\sim$ 35°N). θ and θ_e is represented in z-score due for easier read. TRMM precipitation dataset is left out here because the time-series is available from 1998.

4.4 Summary

We find that the pre-monsoon, meridional, surface θ_e gradient correlates with the monsoon precipitation for Mainland SEA monsoon. The change of surface θ_e spatial pattern corresponds with the change in surface wind and meridional circulation. The zonal-mean precipitation, θ, and θ_e confirms that the Mainland SEA monsoon is a system mixed with moist and dry convection.

THIS PAGE INTENTIONALLY LEFT BLANK

Chapter 5

Conclusions

5.1 Summary of Major Conclusions

In this study, we have analyzed the Mainland SEA monsoon precipitation trends as well as associated surface wind and convection, and evaluated thermal gradient as a part of drivers of the system.

We find that the total precipitation of the Mainland SEA monsoon has experienced a reversing trend from a four-decade-long drying by 0.18 mm day^{-1} decade^{-1} to increasing by 0.13 day^{-1} decade^{-1} starting from 1989. The cross-section wind analysis shows that the Hadley and Walker cell is strengthened post-reversal, bringing more energy and moisture from the seas. The strengthened circulation can be explained by the increasing meridional θ_e gradient. Because θ_e warms faster over land than sea, and the NH is consisting of more land area than SH, the meridional θ_e gradient increases. The meridional θ_e gradient shows significant correlation with the precipitation time-series at r = 0.52 (p = 0.0015), despite θ_e gradient has reversed ahead of precipitation for 4-5 years.

Even though the overall precipitation trend of Mainland SEA in the past decade is increasing, the north of Myanmar and the south of China shows a decreasing trend. The surface wind analysis shows that surface southwesterly wind is weakening in the NH, so the north of Mainland SEA inevitably receives less moisture. On the other hand, the weakening southwesterly allow more moisture from the South China Sea to access the south of Mainland SEA, so the area does not get as dry as the northern part. The weakening of surface southwesterly over SEA also with the rising branch of Hadley cell shifting southward, as shown in meridional, cross-section wind analysis.

Lastly, we find that the Mainland SEA monsoon is a mixed convection system, composing of deep, moist convection directly over the region at 10-20°N, and a shallow, dry convection just north of the region at 35°N, as shown in the meridional, cross-section wind analysis. Further assessment with zonal-mean precipitation, θ, and θ_e confirms that it is a mixed convection system. The deep, moist convection coincides with the zonal-mean θ_e peak, and the strongest convection corresponds with the zonal-mean precipitation peak. The shallow, dry convection coincides with the zonal-mean θ peak at 35°N. The effect of having a mixed convection system is not apparent in this study.

5.2 Implications for Future Work

This study serves as the preliminary research for the Mainland SEA monsoon system. Here, we review some questions for future work to understand the system.

5.2.1 Near-Surface Temperature and Wind Analysis

In this study, we use surface temperature, θ, and θ_e, as well as surface wind to analyze the monsoon system due to its simplicity. However, surface parameters alone do not accurately represent the boundary layer activity and local elevation. Further study that analyzes these parameters using near-surface or boundary-layer parameter instead might yield a clearer and more significant result.

The wind analyses in this study also use rather coarse-resolution wind re-analysis datasets. It might not accurately depict dynamics between land and sea in the region with complicated shoreline such as SEA. Further study using higher-resolution wind datasets would add to the detailed dynamics in the SEA monsoon system.

5.2.2 ENSO and Multi-Decadal Variabilities

In this study, we only look at the meridional thermal gradient as a factor that influenced the precipitation trend. However, other factors must be influencing decadal- and multi-decadal variability in precipitation. There is an apparent decadal-variability in Mainland SEA Monsoon precipitation, such that it introduces complication in analyzing the reversal (the precipitation peak between 1989 and 1999). Other factors that have been shown to correlate with the NH monsoon system are ENSO and Atlantic Multidecadal Oscillation (AMO) (C. Wang, 2015). In Maritime monsoon system, the ENSO has been shown to be a significant interannual and seasonal variability for monsoon rainfall in East Java, Indonesia (Aldrian and Djamil, 2008), and warm ENSO year is found to be associated with monsoon weakening (Moron, Robertson, and Qian, 2010).

5.2.3 Anthropogenic Aerosols and the ITCZ's Southward Shift

As introduced in chapter 3, albeit the overall strengthen change of Hadley circulation, there is a possible south-shift in its rising branch. Globally, the rain band has shown to shift southward due to the spatial distributions of different anthropogenic forcings (C. Wang, 2015; Chung and Soden, 2017). Since the shift seems to be influenced in regional scale, further study in the SEA region on anthropogenic aerosols and the rain band shift could illuminate the reasons or factors behind the change in precipitation trend, and whether the trend will sustain or not. Especially with newly arised concerns of aerosols in SEA urban area, projecting possible variation of precipitation trend due to growing cities are indeed difficult but interesting.

THIS PAGE INTENTIONALLY LEFT BLANK

Bibliography

Adler, Robert F, George J Huffman, Alfred Chang, Ralph Ferraro, Ping-Ping Xie, John Janowiak, Bruno Rudolf, Udo Schneider, Scott Curtis, David Bolvin, et al. (2003). "The version-2 global precipitation climatology project (GPCP) monthly precipitation analysis (1979–present)". *Journal of hydrometeorology* 4.6, pp. 1147–1167.

Aldrian, Edvin and Yudha Setiawan Djamil (2008). "Spatio-temporal climatic change of rainfall in East Java Indonesia". *International Journal of Climatology: A Journal of the Royal Meteorological Society* 28.4, pp. 435–448.

Bollasina, Massimo A, Yi Ming, and V Ramaswamy (2011). "Anthropogenic aerosols and the weakening of the South Asian summer monsoon". *science*, p. 1204994.

Bordoni, Simona and Tapio Schneider (2008). "Monsoons as eddy-mediated regime transitions of the tropical overturning circulation". *Nature Geoscience* 1.8, p. 515.

Byrne, Michael P. and Paul A. O'Gorman (2018). "Trends in continental temperature and humidity directly linked to ocean warming". *Proceedings of the National Academy of Sciences*, pp. 4863–4868. DOI: 10.1073/pnas.1722312115.

Central Intelligent Agency (2018). *The World Factbook*. URL: https://www.cia.gov/library/publications/the-world-factbook/fields/2012.html (visited on 07/22/2018).

Chen, Mingyue, Pingping Xie, John E Janowiak, and Phillip A Arkin (2002). "Global land precipitation: A 50-yr monthly analysis based on gauge observations". *Journal of Hydrometeorology* 3.3, pp. 249–266.

Chung, Eui-Seok and Brian J Soden (2017). "Hemispheric climate shifts driven by anthropogenic aerosol–cloud interactions". *Nature Geoscience* 10.8, p. 566.

Dee, Dick P, S M Uppala, AJ Simmons, Paul Berrisford, P Poli, S Kobayashi, U Andrae, MA Balmaseda, G Balsamo, d P Bauer, et al. (2011). "The ERA-Interim reanalysis: Configuration and performance of the data assimilation system". *Quarterly Journal of the royal meteorological society* 137.656, pp. 553–597.

Harris, IPDJ, Philip D Jones, TJ Osborn, and David H Lister (2014). "Updated high-resolution grids of monthly climatic observations–the CRU TS3. 10 Dataset". *International journal of climatology* 34.3, pp. 623–642.

Held, Isaac M and Brian J Soden (2006). "Robust responses of the hydrological cycle to global warming". *Journal of climate* 19.21, pp. 5686–5699.

Huffman, George J, David T Bolvin, Eric J Nelkin, David B Wolff, Robert F Adler, Guojun Gu, Yang Hong, Kenneth P Bowman, and Erich F Stocker (2007). "The TRMM multisatellite precipitation analysis (TMPA): Quasi-global, multiyear, combined-sensor precipitation estimates at fine scales". *Journal of hydrometeorology* 8.1, pp. 38–55.

Jin, Qinjian and Chien Wang (2017). "A revival of Indian summer monsoon rainfall since 2002". *Nature Climate Change* 7.8, p. 587.

Kalnay, Eugenia, Masao Kanamitsu, Robert Kistler, William Collins, Dennis Deaven, Lev Gandin, Mark Iredell, Suranjana Saha, Glenn White, John Woollen, et al. (1996). "The NCEP/NCAR 40-year reanalysis project". *Bulletin of the American meteorological Society* 77.3, pp. 437–472.

Kiguchi, Masashi, Jun Matsumoto, Shinjiro Kanae, and Taikan Oki (2016). "Pre-Monsoon Rain and Its Relationship with Monsoon Onset over the Indochina Peninsula". *Frontiers in Earth Science* 4, p. 42.

Legates, David R and Cort J Willmott (1990). "Mean seasonal and spatial variability in global surface air temperature". *Theoretical and applied climatology* 41.1-2, pp. 11–21.

Li, Chengfeng and Michio Yanai (1996). "The onset and interannual variability of the Asian summer monsoon in relation to land–sea thermal contrast". *Journal of Climate* 9.2, pp. 358–375.

Loo, Yen Yi, Lawal Billa, and Ajit Singh (2015). "Effect of climate change on seasonal monsoon in Asia and its impact on the variability of monsoon rainfall in Southeast Asia". *Geoscience Frontiers* 6.6, pp. 817–823.

Moron, Vincent, Andrew W Robertson, and Jian-Hua Qian (2010). "Local versus regional-scale characteristics of monsoon onset and post-onset rainfall over Indonesia". *Climate dynamics* 34.2-3, pp. 281–299.

Nie, Ji, William R Boos, and Zhiming Kuang (2010). "Observational evaluation of a convective quasi-equilibrium view of monsoons". *Journal of Climate* 23.16, pp. 4416–4428.

Preethi, B, M Mujumdar, RH Kripalani, Amita Prabhu, and R Krishnan (2017). "Recent trends and tele-connections among South and East Asian summer monsoons in a warming environment". *Climate dynamics* 48.7-8, pp. 2489–2505.

Rayner, NA, De E Parker, EB Horton, CK Folland, LV Alexander, DP Rowell, EC Kent, and A Kaplan (2003). "Global analyses of sea surface temperature, sea ice, and night marine air temperature since the late nineteenth century". *Journal of Geophysical Research: Atmospheres* 108.

Schneider, Udo, Andreas Becker, Peter Finger, Anja Meyer-Christoffer, Markus Ziese, and Bruno Rudolf (2014). "GPCC's new land surface precipitation climatology based on quality-controlled in situ data and its role in quantifying the global water cycle". *Theoretical and Applied Climatology* 115.1-2, pp. 15–40.

Vecchi, Gabriel A, Brian J Soden, Andrew T Wittenberg, Isaac M Held, Ants Leetmaa, and Matthew J Harrison (2006). "Weakening of tropical Pacific atmospheric circulation due to anthropogenic forcing". *Nature* 441.7089, p. 73.

Wang, Bin, Jian Liu, Hyung-Jin Kim, Peter J Webster, So-Young Yim, and Baoqiang Xiang (2013). "Northern Hemisphere summer monsoon intensified by mega-El Niño/southern oscillation and Atlantic multidecadal oscillation". *Proceedings of the National Academy of Sciences* 110.14, pp. 5347–5352.

Wang, Chien (2015). "Anthropogenic aerosols and the distribution of past large-scale precipitation change". *Geophysical research letters* 42.24, pp. 10, 876.

Wang, Huijung (2001). "The weakening of the Asian monsoon circulation after the end of 1970's". *Advances in Atmospheric Sciences* 18.3, pp. 376–386.

Webster, P. J. and J. Fasullo (2003). "Dynamical Theory". *Encyclopedia of Atmospheric Sciences.* University of Colorado Boulder.

Yu, Rucong, Bin Wang, and Tianjun Zhou (2004). "Tropospheric cooling and summer monsoon weakening trend over East Asia". *Geophysical Research Letters* 31.22.